Received: 15 July 2017 | Revised: 31 October 2018 | Accepted: 4 November 2018

DOI: 10.1002/dac.3876

RESEARCH ARTICLE

WILEY

Outage probability bound of decode and forward two-way full-duplex relay employing spatial modulation over cascaded $\alpha - \mu$ channels

Anirban Bhowal | Rakhesh Singh Kshetrimayum

Department of Electronics and Electrical Engineering, IIT Guwahati, Assam, India

Correspondence
Anirban Bhowal, EEE Department, IIT Guwahati, Assam, India.
Email: a.bhowal@iitg.ac.in

Summary

The system performance of mobile-to-mobile (D2D) cooperative communication has been improved by utilizing spatial modulation (SM) in this paper. The proposed system employs decode and forward (DF) relaying technique along with physical layer network coding (PLNC); hence, it has been named as SM-based decode and forward two-way relay (DFTWR). It enables full-duplex communication thereby enhancing the system efficiency. Information bits are exchanged between the two bidirectional nodes. For two bits of information exchange, the antenna index is conveyed by the least significant bit (LSB) of the data symbol while the most significant bit (MSB) carries the message. The system performance has been investigated by analyzing certain performance metrics like lower and upper bounds of outage probability and average data rate for N-α-μ cascaded fading channels. The change in the system performance by varying certain parameters like relative geometrical gain, fading coefficients, and number of cascaded components has also been put forth in this paper.

KEYWORDS

D2D system, N-α-μ cascaded fading channels, outage probability, PLNC, SM

1 | INTRODUCTION

D2D communication is a prevalent research topic that can be utilized for mobile ad hoc networks in wireless communication industry.[1] Cascaded fading models are used as a replacement for old classical models in order to provide better accuracy. In D2D communication, relative motion exists between the transmitter and receiver, and both nodes possess low-height antennas, which are located almost at the street level. Scatterers are also present at transmitter and receiver. D2D communication varies from cellular communication in this aspect. The base station antenna in cellular communication is elevated and fixed, thereby being devoid of local scatterers. However, the mobile antenna is at a lower level and is in motion. Traditional channel models are unsuitable for D2D communication as multiple scattering groups are present in D2D communication.[2]

Abbreviations: D2D, device to device; PLNC, physical layer network coding; SM, spatial modulation

Previous works list out several 2D and 3D channel models.[3-8] The major concern with these models is that a solitary or dual scattering group is considered in a majority of these models, whereas multiple scattering groups are present in reality. Hence, in such scenarios, cascaded model is more suitable.

Previous researches have incorporated the utilization of N-Nakagami fading channel model[9] and cascaded Rayleigh fading channel models.[10] Weibull channel can be more appropriate for D2D communication[11] as it generates more deeper fades than conventional Nakagami and Rayleigh channel. Weibull channel describes a particular example of the N-α-μ channel model where the corresponding parameters are N = 1 and $\mu = 1$. Leonardo and Yacoub[12,13] have proposed N-α-μ channel model, and it is a generalized version of the N-Nakagami model. Cooperative communication with various protocols is implemented in D2D communication to provide good quality coverage and higher data rates. Decode and forward (DF), a type of relaying protocol, has been used by Gong et al[14] over double Nakagami (a specialized case of N-Nakagami channel) fading channels. Incremental amplify and forward (AF) protocol for D2D cooperative communication has been implemented, and evaluation of outage probability has been achieved in Xu et al.[15] Cascaded α-μ distribution has been explained in Leonardo and Yacoub,[12] and derivation of formulae for probability density function (PDF) and cumulative distribution function (CDF) has been done by the authors. But performance evaluation for SM-based relay D2D model is yet to be achieved using this cascaded model.

One of the generalized physical fading models is the α-μ fading model consisting of multipath clusters propagating in a nonhomogeneous environment.[16-18] Two variables are used to normally characterize it—α and μ. The propagation medium has a nonlinearity index that is depicted by α, whereby μ indicates the count of the multipath clusters. Rayleigh, Gamma, and Nakagami distributions are some of the specialized cases of α-μ distribution. In literature, Fox H function has been utilized to describe a cascaded α-μ model.[19] But because of the mathematical complexities, Meijer G function is a better option because of its ease of availability in software packages like Mathematica and Matlab. Moment-generating function (MGF) can be utilized to compute the PDF and CDF for cascaded channel models. The cascaded α-μ distribution has been utilized in this paper whose PDF and CDF have been evaluated by using the scheme of multiplication of random variables.

In this paper, SM along with PLNC[20] has been used for full-duplex communication. This will result in greater data rate and bandwidth efficiency. In normal nonnetwork coding scheme, exchange of two packets takes four time slots to avoid collision. Analog network coding scheme (ANC) uses three time slots to complete the same operation by pairwise XOR-ing of the symbols over the two sources. In PLNC,[21] time slots required to achieve the same operation is two only. This is due to the network coding scheme implemented automatically in the superimposed electromagnetic (EM) waves. At the relay, the symbol is decoded using mapping scheme. The proposed system evaluates the performance of D2D cooperative system using DF and SM technique. This will reduce the inter-antenna interference and also exploits the natural mixing of signals because of superposition of EM waves coming from two different sources.

PLNC[22-24] has been used effectively for classical channel models in previouse studies.[25-27] Yang et al[25] have used techniques like transmit and receive beamforming and transmit and receive antenna selection for performance evaluation of PLNC over relay-based system. Bounds for outage probability and diversity order has been calculated for independent but not necessarily identical Nakagami distribution. Nasab et al[26] have used PLNC over K relays with two antennas in each relay and analyzed system performance over iid Nakagami-m fading channels. In Nasab et al,[27] transmit and receive antenna selection has been used.

The idea of SM stems from the fact that simultaneous usage of multiple radio frequency (RF) chains both at the transmiter and receiver in PLNC system leads to unnecessary power consumption and escalates the system cost considerably. Also, there will be inter-antenna interference because of the use of multiple RF chains for several antennas simultaneously. This can be overcome by SM technique where a single RF chain with a single antenna will be active at a time depending on the selected transmit antenna index. In SM, information is divided into two portions—one is mapped to a symbol using a particular constellation scheme, and the other is used for activating the transmit antenna.[28,29]

The bounds on outage probability, both at lower and upper levels, and average data rate for D2D relay system have been evaluated and compared with other techniques available in literature. Monte Carlo simulations have been implemented for various channel parameters to determine the validity of the analytical method. The effect of different channel parameters on the system performance has been investigated and presented in this work.

Section 2 lists the details of N-α-μ fading channel distribution along with all mathematical expressions. Section 3 vividly illustrates the proposed system model, whereas the performance analysis with respect to average data rate and outage probability has been illustrated in Section 4. The analytical results along with its validation through simulation results have been explained in Section 5, while conclusion has been drawn in Section 6.

2 | PDF AND CDF OF CASCADED α-μ CHANNEL COEFFICIENTS

Let the random variable $\varrho \geq 0$ be the signal envelope of α-μ distribution[12]:

$$f_{\varrho}(\rho) = \frac{\alpha \mu^{\mu} \rho^{\alpha\mu-1}}{\Gamma(\mu)\hat{\rho}^{\alpha\mu} exp[-\mu(\frac{\rho}{\hat{\rho}})^{\alpha}]} \quad , \tag{1}$$

where $\alpha > 0$ signifies parameter of nonlinearity, Gamma function is depicted by Γ, the count of multipath clusters is denoted by $\mu > 0$, and $\hat{\rho} = \sqrt[\alpha]{E(\varrho^{\alpha})}$. Let $\varrho_1, \varrho_2, \ldots, \varrho_n$ be $n \geq 2$ positive random variables, which are statistically independent in nature, and $Z_n = \prod_{i=1}^{n} \varrho_i$ be their product. So PDF $f_{Z_n}(z)$ has to be evaluated to obtain the PDF of cascaded $\alpha - \mu$ channel coefficients. Hence, the PDF of cascaded α-μ distribution can be expressed as[12]:

$$f_{Z_n}(z) = \frac{(2\pi)^{(\frac{N-v_s}{2})} u v_p}{\Gamma(\mu) h_p^{\alpha_1} z^{\alpha_1+1}} G_{0,v_s}^{v_s,0}\left[\frac{-}{b}\middle|\frac{(h_p z)^u}{v_e}\right] \quad , \tag{2}$$

where $G_{0,v_s}^{v_s,0}(:|\ z)$ is popularly known as the Meijer G function.[30,31] The derivations have been explained in details in Leonardo and Yacoub.[12,13] To evaluate the integral, certain assumptions have to be considered. The ratio of $r = \frac{\alpha_1}{\alpha_j} = \frac{p_j}{q_j}$ has been assumed where the two variables $p_j \geq 1$ and $q_j \geq 1$ are considered to be coprime integers, $j = 2, \ldots N$. The count of cascaded components is denoted by N. Here, r is the ratio between the α of the first channel and the α of the jth channel. The variables in (2) are defined as

$$h_i = \frac{\mu_i^{\frac{1}{\alpha_i}}}{\hat{\rho}_i}, \quad h_p = \prod_{l=1}^{N} h_i, \quad v_1 = \prod_{l=2}^{N} q_i, \quad v_l = \frac{p_l}{q_l} v_1,$$
$$v_s = \sum_{l=1}^{N} v_l, \quad v_e = \prod_{l=1}^{N} v_l^{v_l}, \quad v_{\sigma} = \prod_{l=1}^{N} v_l^{\mu_l + \frac{\alpha_1}{\alpha_l} - \frac{1}{2}},$$
$$u = \alpha_1 v_1 = \alpha_2 v_2 = \ldots\ldots = \alpha_n v_n, \qquad \Gamma_{\mu} = \prod_{l=1}^{N} \Gamma(\mu_l),$$
$$b^{(i)} = \Delta(v_i, \mu_i + \frac{\alpha_1}{\alpha_i}), b = b^{(1)}, b^{(2)}, \ldots, b^{(n)}, \text{ and}$$
$$\Delta(k, a) = \frac{a}{k}, \frac{a+1}{k}, \ldots\ldots, \frac{a+k-1}{k}.$$

Equation 2 is integrated to obtain the CDF and is written as in[12,13]

$$F_{Z_n}(z) = \frac{(2\pi)^{(\frac{N-v_s}{2})} v_p}{\Gamma(\mu)(h_p z)^{\alpha_1}} G_{1,v_s+1}^{v_s,1}\left[\frac{\frac{1}{v_1}+1}{b, \frac{1}{v_1}}\middle|\frac{(h_p z)^u}{v_e}\right] \quad . \tag{3}$$

3 | PROPOSED MODEL

Figure 1 depicts a simple three-node bidirectional cooperative model, where the two mobile source nodes (MS1 and MS2) exchange information through a mobile relay node (MR) located in between the two source nodes. This is the system model that has been proposed for this paper. All the nodes are spatially modulated full-duplex (SMFD) nodes with N_A antennas. To mitigate self interference, it is considered that the nodes have independent RF chains for transmission and reception purpose. For this proposed system, each source node exchanges bits of data with the other source node using PLNC at the relay employing DF technique. All the links have corresponding relative gains,[32,33] which can be expressed as $G_{S_1R} = (\frac{d_{SD}}{d_{SR}})^{\tau}$, $G_{S_2R} = (\frac{d_{SD}}{d_{RD}})^{\tau}$, where the relative gain of MS1 to MR link is denoted by G_{S_1R} while the relative gain of MR to MS2 link is denoted by G_{S_2R}, and τ is the coefficient of path loss, d_{SD}, d_{SR}, and d_{RD}, which are the distances between MS1 and MS2, MS1 and MR, and MR and MS2 links, respectively. Relative geometrical gain factor $\kappa = \frac{G_{S_1R}}{G_{S_2R}}$ indicates the position of MR node as compared with the locations of MS1 and MS2 nodes. κ, when expressed in dB, is negative if $d_{RD} < d_{SR}$, whereas κ is positive in dB if $d_{RD} > d_{SR}$, and if both distances are equal, then κ is 0 dB.

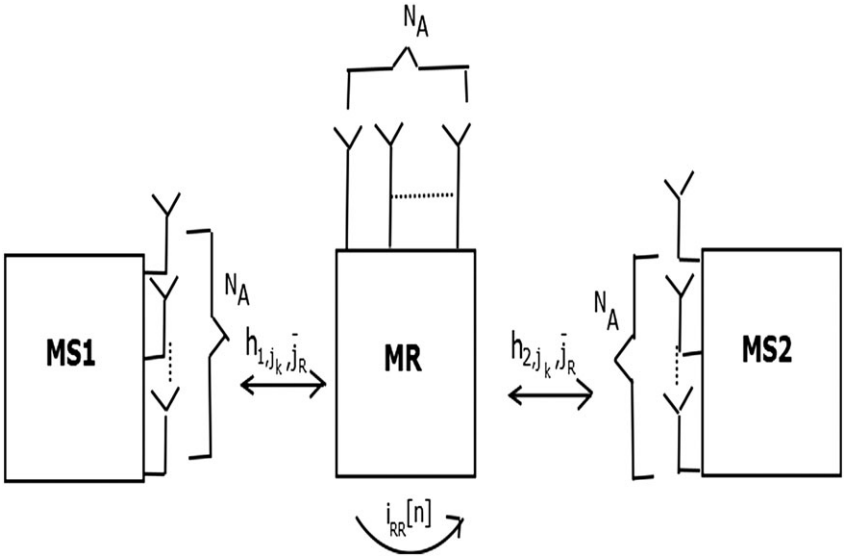

FIGURE 1 Proposed system model

TABLE 1 Spatial modulation for $N_A = 4$

Input Bits	Antenna Index	BPSK Symbol
000	1	−1
001	2	−1
010	3	−1
011	4	−1
100	1	1
101	2	1
110	3	1
111	4	1

For $N_A = 2$, the transmit antenna, which is made active, is chosen as

$$j_k = \begin{cases} 2, \text{ if } c_k^{LSB}[n] = 1 \\ 1, \text{ if } c_k^{LSB}[n] = 0 \end{cases} , \tag{4}$$

where n represents the nth time slot and k indicates the source node, which may be 1 or 2 in this case. $c_k[n]$ represents the bits, which may be 0 or 1 for BPSK (binary phase shift keying). If $N_A > 2$, then $log_2 N_A$ number of bits (from LSB side) will be used for transmit antenna activation, and $log_2 M$ message bit will be used for M-ary modulation scheme. Note that $N_A = 2^n$ where n is any integer and $n = 1, 2, 3, \ldots$. We will consider BPSK modulation scheme for our case. The table of antenna activation depending upon the message bits has been listed in Tables 1 and 2 for $N_A = 4$ and $N_A = 8$, respectively.

Both the sources transmit data to relay node simultaneously using BPSK as

$$x_k^{MSB}[n] = 2c_k^{MSB}[n] - 1 \quad , \tag{5}$$

where $k = 1, 2$. At the relay node, the signal received in nth time slot at the $\bar{j_R}$ antenna is computed as

$$y_R^{\bar{j_R}}[n] = \sum_{k=1}^{2} \sqrt{P_k G_{S_k,R}} \quad h_{k,j_k,\bar{j_R}} x_k^{MSB}[n] + i_{RR}[n] + w_R[n] \quad . \tag{6}$$

Suppose j_k is the selected transmit antenna from which message would be transmitted at the source node and $\bar{j_R}$ is the selected receive antenna at the relay node. Then $|h_{k,j_k,\bar{j_R}}|$ represents cascaded α-μ channel coefficients between the selected transmit and receive antenna at the source and relay nodes, respectively. The variables with a bar indicate receive antenna while those without bar indicate transmit antenna. P_k indicates the power of transmission at the source nodes S_k, k=1, 2. $w_R[n]$ represents complex Gaussian random noise with variance N_0 and a mean of zero at relay node MR . The relay node, undergoing full-duplex operation, suffers from self interference indicated by $i_{RR}[n]$. The term is described as Gaussian

TABLE 2 Spatial modulation for $N_A = 8$

Input Bits	Antenna Index	BPSK Symbol
0000	1	−1
0001	2	−1
0010	3	−1
0011	4	−1
0100	5	−1
0101	6	−1
0110	7	−1
0111	8	−1
1000	1	1
1001	2	1
1010	3	1
1011	4	1
1100	5	1
1101	6	1
1110	7	1
1111	8	1

random variable with zero mean and power $I_R = N_0[10^{\beta/10} - 1], \beta \geq 0$ where the signal to noise ratio (SNR) loss factor in dB is denoted by β.[34] The parameters $j_1, j_2, x_1^{MSB}[n]$, and $x_2^{MSB}[n]$ are obtained by applying the principle of maximum likelihood (ML) detection[35] and can be estimated as $\hat{j}_1, \hat{j}_2, \hat{x}_1^{MSB}[n]$, and $\hat{x}_2^{MSB}[n]$ respectively, as shown below:

$$(\hat{j}_1, \hat{j}_2, \hat{x}_1^{MSB}[n], \hat{x}_2^{MSB}[n]) = \underset{(j_1, j_2, x_1^{MSB}[n], x_2^{MSB}[n])}{min} \left| y_R^{\bar{j}_R}[n] - \sum_{k=1}^{2} \sqrt{P_k G_{S_k,R}} h_{k,j_k,\bar{j}_R} x_k^{MSB}[n] \right|^2 \quad . \tag{7}$$

The transmit antenna selection is done according to the formula $j_R = \hat{j}_1 \oplus \hat{j}_2$. For bitwise XOR operation, the antenna index would be coded, for example, in case of $N_A = 2$, antenna index 1 would be denoted by 0 and antenna index 2 would be denoted by 1. The encoded symbol forwarded by the relay to the source nodes is given by

$$x_R^{MSB}[n] = \hat{x}_1^{MSB}[n] \oplus \hat{x}_2^{MSB}[n] \quad . \tag{8}$$

The source nodes receive the signals, which are given by

$$y_k^{\bar{j}_k} = \sqrt{P_R G_{S_k,R}} \quad h_{k,\bar{j}_k,j_R} x_R^{MSB}[n] + i_{kk}[n] + w_k[n], \quad k = 1, 2 \quad . \tag{9}$$

$w_k[n]$ represents complex Gaussian random noise with variance N_0 and a mean of zero at source node S_k . The particular source node, because of its full-duplex nature, undergoes self interference, which is indicated by $i_{kk}[n]$. This term is described as Gaussian random variable with zero mean and power $I_k = N_0[10^{\beta/10} - 1], \beta \geq 0$ where the SNR loss factor in dB is denoted by β, as described earlier. Assuming that the source nodes have knowledge about channel state information (CSI), the parameters $j_R, x_R^{MSB}[n]$ are detected at the source nodes using maximum likelihood (ML) method and can be estimated as $\hat{j}_R$ and $\hat{x}_R^{MSB}$, respectively.

$$(\hat{j}_R, \hat{x}_R^{MSB}[n]) = \underset{(j_R, x_R^{MSB}[n])}{min} \left| y_k^{\bar{j}_k}[n] - \sqrt{P_R G_{S_k,R}} h_{k,\bar{j}_k,j_R} x_R^{MSB}[n] \right|^2 \quad . \tag{10}$$

The source nodes already have the values of j_k and $x_k^{MSB}[n]$ as they transmit the respective bits. Hence, the bits estimated at the kth source node are denoted by $\hat{x}_k^{MSB}$ and $\hat{x}_k^{LSB}$.

$$\hat{x}_k^{LSB}[n] = \hat{j}_R \oplus j_k \quad k = 1, 2 \quad , \tag{11}$$

$$\hat{x}_k^{MSB}[n] = \hat{x}_R^{MSB}[n] \oplus x_k^{MSB}[n], \quad k = 1, 2 \quad . \tag{12}$$

4 | PERFORMANCE ANALYSIS

Derivations for analytical expressions of outage probability bounds have been performed and verified in this section.

4.1 | Lower bound of outage probability

Assume $\eta_k = \frac{P_k}{N_0}$ be the source node SNR while $\eta_R = \frac{P_R}{N_0}$, $k = 1, 2$ be the SNR at mobile relay (MR) node. The $\bar{j}_R$ antenna of MR node will possess a signal to interference plus noise ratio (SINR), which can be evaluated as

$$\gamma_{S_k,R}^{\bar{j}_R} = \frac{\eta_k G_{S_k,R} |h_{k,j_k,\bar{j}_R}|^2}{\frac{I_R}{N_0} + 1}, \qquad k = 1, 2 \quad . \tag{13}$$

The source node S_k will have a SINR, which can be evaluated as

$$\gamma_{R,S_k,}^{\bar{j}_k} = \frac{\eta_R G_{S_k,R} |h_{k,\bar{j}_k,j_R}|^2}{\frac{I_R}{N_0} + 1}, \qquad k = 1, 2 \quad . \tag{14}$$

The outage probability of the SM-based DFTWR system will be bounded at a lower level for a data rate of R_d bits/s, which can be defined as

$$P_{out}^{RLB}(R_d) = P_r[2log_2(N_A) + log_2(1 + min(max(\gamma_{S_1,R}^1, \gamma_{S_1,R}^2, \ldots, \gamma_{S_1,R}^{N_A}), max(\gamma_{S_2,R}^1, \gamma_{S_2,R}^2, \ldots, \gamma_{S_2,R}^{N_A}))) < R_d] \quad . \tag{15}$$

The prelog term $2log_2(N_A)$ is used because of the capacity generated due to the spatial domain part.[36] Assuming there is no error in estimating the transmitting antenna, $log_2(N_A)$ bits are used for activating the antenna, and since the system is bidirectional, the term is multiplied by 2. The max-min criteria has been used for selecting the optimum SNR for lower bound in this case.[37,38] Assume $\psi_R = min\left(max\left(\gamma_{S_1,R}^0, \gamma_{S_1,R}^1, \ldots, \gamma_{S_1,R}^{N_A}\right), max\left(\gamma_{S_2,R}^1, \gamma_{S_2,R}^2, \ldots, \gamma_{S_2,R}^{N_A}\right)\right)$, and $\gamma_{th} = 2^{R_d - 2*log_2(N_A)} - 1$. In this case, $N_A = 2$. Hence, the outage probability can be rewritten as

$$P_{out}^{RLB}(\gamma_{th}) = P_r[\psi_R \leq \gamma_{th}] \quad . \tag{16}$$

The CDF of ψ_R is written as

$$\begin{aligned}
F_{\psi_R}(\gamma th) &= P\left\{ min\left[max(\gamma_{S_1,R}^1, \gamma_{S_1,R}^2, \cdots, \gamma_{S_1,R}^{N_A}), max(\gamma_{S_2,R}^1, \gamma_{S_2,R}^2, \cdots, \gamma_{S_2,R}^{N_A}) \right] \leq \gamma_{th} \right\} \\
&= 1 - P\left\{ min\left[max(\gamma_{S_1,R}^1, \gamma_{S_1,R}^2, \cdots, \gamma_{S_1,R}^{N_A}), max(\gamma_{S_2,R}^1, \gamma_{S_2,R}^2, \cdots, \gamma_{S_2,R}^{N_A}) \right] > \gamma_{th} \right\} \\
&= 1 - P(max(\gamma_{S_1,R}^1, \gamma_{S_1,R}^2, \cdots, \gamma_{S_1,R}^{N_A}) > \gamma_{th}) P(max(\gamma_{S_2,R}^1, \gamma_{S_2,R}^2, \cdots, \gamma_{S_2,R}^{N_A}) > \gamma_{th}) \\
&= 1 - \left[\left\{ 1 - P(max(\gamma_{S_1,R}^1, \gamma_{S_1,R}^2, \cdots, \gamma_{S_1,R}^{N_A}) \leq \gamma_{th}) \right\} \right. \\
&\quad \left. \left\{ 1 - P(max(\gamma_{S_2,R}^1, \gamma_{S_2,R}^2, \cdots, \gamma_{S_2,R}^{N_A}) \leq \gamma_{th}) \right\} \right] \\
&= 1 - \left[\left\{ 1 - P(\gamma_{S_1,R}^1 \leq \gamma_{th}) P(\gamma_{S_1,R}^2 \leq \gamma_{th}) \ldots P(\gamma_{S_1,R}^{N_A} \leq \gamma_{th}) \right\} \right. \\
&\quad \left. \left\{ 1 - P(\gamma_{S_2,R}^1 \leq \gamma_{th}) P(\gamma_{S_2,R}^2 \leq \gamma_{th}) \ldots P(\gamma_{S_2,R}^{N_A} \leq \gamma_{th}) \right\} \right] \\
&= 1 - \prod_{k=1}^{2} (1 - F_{\gamma_{S_k,R}^1}(\gamma_{th}) F_{\gamma_{S_k,R}^2}(\gamma_{th}), \cdots, F_{\gamma_{S_k,R}^{N_A}}(\gamma_{th})) \quad .
\end{aligned} \tag{17}$$

By referring to Equation 13, the CDF of SINR can be computed as

$$\begin{aligned}
F_{\gamma_{S_k,R}^{\bar{j}_R}}(\gamma th) &= P_r\left[\frac{\eta_k G_{S_k,R} |h_{k,j_k,\bar{j}_R}|^2}{\frac{I_R}{N_0} + 1} \leq \gamma_{th} \right], \\
\bar{j}_R &= 1, 2, \ldots N_A, \quad k = 1, 2.
\end{aligned} \tag{18}$$

$|h_{k,j_k,\bar{j_R}}|$ follows cascaded α-μ distribution, as given in Equation 2, with $N = 2$. Let $y = \left|h_{k,j_k,\bar{j_R}}\right|^2$. After taking into consideration the change of random variable (RV), the PDF of y is evaluated as[39]

$$f_Y(y) = \frac{(2\pi)^{\left(\frac{N-v_s}{2}\right)} u v_p}{2\Gamma(\mu) h_p^{\alpha_1} y^{\frac{\alpha_1}{2}+1}} G_{0,v_s}^{v_s,0}\left[\frac{-}{b}\middle| \frac{h_p{}^u y^{\frac{u}{2}}}{v_e}\right] \quad . \tag{19}$$

The PDF is integrated to obtain the corresponding CDF, which can be written as[39]

$$F_Y(y) = \frac{(2\pi)^{\left(\frac{N-v_s}{2}\right)} v_p}{\Gamma(\mu) h_p{}^{\alpha_1} y^{\frac{\alpha_1}{2}}} G_{1,v_s+1}^{v_s,1}\left[\frac{\frac{1}{v_1}+1}{b, \frac{1}{v_1}}\middle| \frac{h_p{}^u y^{\frac{u}{2}}}{v_e}\right] \quad . \tag{20}$$

Using Equations 13, 18, and 20, we can write

$$F_{\gamma_{S_k,R}^{\bar{j_R}}}(\gamma_{th}) = \frac{(2\pi)^{\left(\frac{N-v_s}{2}\right)} v_p}{\Gamma(\mu) h_p{}^{\alpha_1} (\gamma_{th}\beta_{abs}/(\eta_k G_{S_k,R}))^{\frac{\alpha_1}{2}}} G_{1,v_s+1}^{v_s,1}\left[\frac{\frac{1}{v_1}+1}{b, \frac{1}{v_1}}\middle| \frac{h_p{}^u (\gamma_{th}\beta_{abs}/\left(\eta_k G_{S_k,R}\right))^{\frac{u}{2}}}{v_e}\right] \quad , \tag{21}$$

where $\beta_{abs} = 10^{\beta/10}$. The values obtained from Equation 21 is put into Equation 17 to compute $F_{\psi_R}(\gamma_{th})$. Now, the source node S_k (k=1, 2) will have an outage probability that can be computed as[38]

$$P_{out}^{S_k}(R_d) = P_r\left[2log_2(N_A) + log_2\left(1 + min\left(\gamma_{R,S_k}^1, \gamma_{R,S_k}^2, \ldots, \gamma_{R,S_k}^{N_A}\right)\right) < R_d\right], \quad k = 1, 2 \quad . \tag{22}$$

The prelog term is used because of the same reason as explained earlier in Equation 15. Assume $\psi_{S_k} = min(\gamma_{R,S_k}^1, \gamma_{R,S_k}^2, \ldots, \gamma_{R,S_k}^{N_A})$. Thus, the outage probability can be expressed as

$$P_{out}^{S_k}(\gamma_{th}) = P_r[\psi_{S_k} \le \gamma_{th}], \quad k = 1, 2 \quad . \tag{23}$$

The CDF of ψ_{S_k} is written as

$$\begin{aligned} F_{\psi_{S_k}}(\gamma_{th}) &= P\left\{min(\gamma_{R,S_k}^1, \gamma_{R,S_k}^2, \ldots, \gamma_{R,S_k}^{N_A}) \le \gamma_{th}\right\} \\ &= 1 - P\left\{min(\gamma_{R,S_k}^1, \gamma_{R,S_k}^2, \ldots, \gamma_{R,S_k}^{N_A}) > \gamma_{th}\right\} \\ &= 1 - P\left(\gamma_{R,S_k}^1 > \gamma_{th}\right) P\left(\gamma_{R,S_k}^2 > \gamma_{th}\right) \ldots P\left(\gamma_{R,S_k}^{N_A} > \gamma_{th}\right) \\ &= 1 - \left[\left(1 - P\left\{\gamma_{R,S_k}^1 \le \gamma_{th}\right\}\right)\left(1 - P\left(\gamma_{R,S_k}^2 \le \gamma_{th}\right)\right) \ldots \left(1 - P\left(\gamma_{R,S_k}^{N_A} \le \gamma_{th}\right)\right)\right] \\ &= 1 - \prod_{\bar{j_k}=1}^{N_A}\left(1 - F_{\gamma_{R,S_k}^{\bar{j_k}}}(\gamma_{th})\right), \quad k = 1, 2 \quad . \end{aligned} \tag{24}$$

By referring to Equation 14, the CDF of SINR can be computed as

$$\begin{aligned} F_{\gamma_{R,S_k}^{\bar{j_k}}}(\gamma th) = P_r\left[\frac{\eta_R G_{S_k,R}\left|h_{k,\bar{j_k},j_R}\right|^2}{\frac{I_R}{N_0}+1} \le \gamma_{th}\right], \\ k = 1, 2, \bar{j_k} = 0, 1, \ldots, N_A \quad . \end{aligned} \tag{25}$$

$|h_{k,\bar{j_k},j_R}|$ follows cascaded α-μ distribution, as given in Equation 2, with $N = 2$. Let $y = |h_{k,\bar{j_k},j_R}|^2$. After taking into consideration the change of random variable (RV), the PDF of y can be written as shown in Equation 19. Again, using Equations 14 and 20, we can write CDF of SINR as

$$F_{\gamma_{R,S_k}^{\bar{j_k}}}(\gamma_{th}) = \frac{(2\pi)^{\left(\frac{N-vs}{2}\right)} v_p}{\Gamma(\mu) h_p{}^{\alpha_1} (\gamma_{th}\beta_{abs}/(\eta_R G_{S_k,R}))^{\frac{\alpha_1}{2}}} G_{1,v_s+1}^{v_s,1}\left[\frac{\frac{1}{v_1}+1}{b, \frac{1}{v_1}}\middle| \frac{h_p{}^u (\gamma_{th}\beta_{abs}/\left(\eta_R G_{S_k,R}\right))^{\frac{u}{2}}}{v_e}\right] \quad , \tag{26}$$

where depending upon the value of k, $G_{S_1,R}$ or $G_{S_2,R}$ is chosen. The values obtained from Equation 26 is put into Equation 24 to obtain $F_{\psi_k}(\gamma_{th})$. The total system outage probability can be computed by taking into account the outage probabilities at the source and relay nodes. The terms obtained from Equations 17 and 24 are used, and the final outage probability is expressed as

$$\begin{aligned} P_{out}^{LB}(\gamma_{th}) &= P_{out}^{RLB}(\gamma_{th}) + (1 - P_{out}^{RLB}(\gamma_{th}))P_{out}^{S_k}(\gamma_{th}) \\ &= 1 - \prod_{k=1}^{2}(1 - F_{\gamma_{S_k,R}^1}(\gamma_{th})F_{\gamma_{S_k,R}^2}(\gamma_{th}), \ \dots, F_{\gamma_{S_k,R}^{N_A}}(\gamma_{th})) \\ &\quad + \left[\prod_{k=1}^{2}(1 - F_{\gamma_{S_k,R}^1}(\gamma_{th})F_{\gamma_{S_k,R}^2}(\gamma_{th}), \ \dots, F_{\gamma_{S_k,R}^{N_A}}(\gamma_{th}))\right] \\ &\quad \text{x} \left[1 - \prod_{\bar{j}_k=1}^{N_A}(1 - F_{\gamma_{R,S_k}^{\bar{j}_k}}(\gamma_{th}))\right] \\ &= 1 - \left[\prod_{k=1}^{2}(1 - F_{\gamma_{S_k,R}^1}(\gamma_{th})F_{\gamma_{S_k,R}^2}(\gamma_{th}), \ \dots, F_{\gamma_{S_k,R}^{N_A}}(\gamma_{th}))\right] \\ &\quad \text{x} \left[\prod_{\bar{j}_k=1}^{N_A}(1 - F_{\gamma_{R,S_k}^{\bar{j}_k}}(\gamma_{th}))\right] \quad . \end{aligned} \tag{27}$$

The total transmission comprises of two phases. The first phase involves message transmission to the relay from the source nodes for which the term P_{out}^{RLB} defines the outage probability of the first phase. The second phase is the broadcasting stage from the relay. The second term in Equation 27 given by $(1-P_{out}^{RLB}(\gamma_{th}))P_{out}^{S_k}(\gamma_{th})$ yields the outage probability for this phase.

In Equation 27, we can observe that the term $F_{\gamma_{R,S_k}^{\bar{j}_k}}(\gamma_{th})$ does not vary with SNR as η_R is fixed. So the outage probability depends on the term $F_{\gamma_{S_k,R}^{\bar{j}_R}}(\gamma_{th})$. This term contains the Meijer G function, as can be seen from Equation 21, which depends on the SNR η_k. As SNR increases, the Meijer G function decreases resulting in a decrease in value of the overall term $F_{\gamma_{S_k,R}^{\bar{j}_R}}(\gamma_{th})$. Hence, the product of such terms also decreases. The subtraction of the resulting product term from 1 gives an increase in the result, which is again subtracted from 1, thereby causing an overall decrease in the outage probability value with increase in SNR.

4.2 | Upper bound of outage probability

Now, the SM-based DFTWR system will have its outage probability bounded at an upper level for a data rate of R_d bit/s, which can be defined as

$$P_{out}^{RUB}(R_d) = P_r[2log_2(N_A) + log_2(1 + min(\gamma_{S_1,R}^1, \gamma_{S_1,R}^2, \cdots, \gamma_{S_1,R}^{N_A}, \gamma_{S_2,R}^1, \gamma_{S_2,R}^2, \cdots, \gamma_{S_2,R}^{N_A})) < R_d] \quad . \tag{28}$$

The other steps would remain the same as that of lower bound computation. The minimum SNR has to be chosen for the upper bound as explained in Liu et al.[38] Assume $\psi_{S_k} = min(\gamma_{S_1,R}^1, \gamma_{S_1,R}^2, \cdots, \gamma_{S_1,R}^{N_A}, \gamma_{S_2,R}^1, \gamma_{S_2,R}^2, \cdots, \gamma_{S_2,R}^{N_A})$ and $\gamma_{th} = 2^{R_d - 2*log_2(N_A)} - 1$.

$$\begin{aligned} P_{out}^{RUB}(\gamma_{th}) &= F_{\psi_{S_k}}(\gamma_{th}) \\ &= P\left\{min(\gamma_{S_1,R}^1, \gamma_{S_1,R}^2, \cdots, \gamma_{S_1,R}^{N_A}, \gamma_{S_2,R}^1, \gamma_{S_2,R}^2, \cdots, \gamma_{S_2,R}^{N_A}) \le \gamma_{th}\right\} \\ &= 1 - \prod_{k=1}^{2}\left(\prod_{\bar{j}_R=1}^{N_A}\left(1 - F_{\gamma_{S_k,R}^{\bar{j}_R}}(\gamma_{th})\right)\right), \qquad \bar{j}_R = 1, 2, \cdots, N_A, \quad k = 1, 2 \quad , \end{aligned} \tag{29}$$

where $F_{\gamma_{S_k,R}^{\bar{j}_R}}(\gamma_{th})$ is defined in Equation 21. So the total outage probability upper bound, after using the terms from Equations 29 and 24, can be defined as

$$
\begin{aligned}
P_{out}^{UB}(\gamma_{th}) &= P_{out}^{RUB}(\gamma_{th}) + (1 - P_{out}^{RUB}(\gamma_{th}))P_{out}^{S_k}(\gamma_{th}) \\
&= 1 - \prod_{k=1}^{2}(\prod_{\tilde{j}_R=1}^{N_A}(1 - F_{\gamma_{S_k,R}^{\tilde{j}_R}}(\gamma_{th}))) + \left[\prod_{k=1}^{2}(\prod_{\tilde{j}_R=1}^{N_A}(1 - F_{\gamma_{S_k,R}^{\tilde{j}_R}}(\gamma_{th}))\right] \\
&\quad \text{x} \left[1 - \prod_{\tilde{j}_k=1}^{N_A}(1 - F_{\gamma_{R,S_k}^{\tilde{j}_k}}(\gamma_{th}))\right] = 1 - \left[\prod_{k=1}^{2}(\prod_{\tilde{j}_R=1}^{N_A}(1 - F_{\gamma_{S_k,R}^{\tilde{j}_R}}(\gamma_{th})))\right] \\
&\quad \text{x} \left[\prod_{\tilde{j}_k=1}^{N_A}(1 - F_{\gamma_{R,S_k}^{\tilde{j}_k}}(\gamma_{th}))\right] \quad ,
\end{aligned} \tag{30}
$$

where the term $F_{\gamma_{R,S_k}^{\tilde{j}_k}}(\gamma_{th})$ can be obtained from Equation 26. During the first phase, message is transmitted by the source nodes to the relay, and the term P_{out}^{RUB} defines the outage probability for this phase. The second phase is the broadcasting stage from the relay. The second term in Equation 30 given by $(1 - P_{out}^{RUB}(\gamma_{th}))P_{out}^{S_k}(\gamma_{th})$ yields the outage probability for this phase.

4.3 | Average data rate

The average data rate for this proposed system is computed and compared with other existing models. Amplify and forward two-way relaying (AFTWR), amplify and forward one-way relaying (AFOWR), ANC, and PLNC are the methods available in literature. Average data rate of the proposed system deploying DF relaying technique can be written as

$$
\bar{R} = E[2log_2(N_A) + log_2(1 + min(max(\gamma_{S_1,R}^1, \gamma_{S_1,R}^2, \cdots, \gamma_{S_1,R}^{N_A}), max(\gamma_{S_2,R}^1, \gamma_{S_2,R}^2, \cdots, \gamma_{S_2,R}^{N_A})))] \quad , \tag{31}
$$

where E[ ] denotes expectation. All the terms have been explained while deriving lower bound expression.

In AFTWR, the system performance is worse than AFOWR because of the presence of self-interference because in AFTWR, the source and relay nodes transmit and receive messages simultaneously, but in case of AFOWR, only the relay operates in full-duplex mode. The average date rates of the systems are defined in Zhang et al.[40]

5 | RESULTS AND DISCUSSION

In this section, bounds on outage probability have been plotted analytically for various system parameters, and the results have been validated by Monte Carlo simulations. All the nodes have been assumed to have two antennas, ie, $N_A = 2$. The parameters considered are $\beta = 0$ dB, $N = 2$, $r = 1$, and $\kappa = 0$ dB for all cases unless explicitly specified.

The proposed system is investigated according to performance metric of outage probability, and comparison has been done with the methods existing in literature by evaluating all the lower bounds. It is evident from Figure 2 that outage probability value is least for SM-based DFTWR (DFTWR_SM) followed by AFOWR, PLNC, AFTWR, and ANC. It is clearly evident that the simulation results follow a tight lower bound for the proposed method, thereby validating our analysis. The parameters used for comparison are $\beta = 0$ dB and $N = 2$ while $\eta_R = \eta_k$.

The different SNR values required to achieve certain target outage probability values for different methods have been tabulated in Table 3. Three different target outage probability values are chosen as 0.1, 0.05, and 0.03. It is evident from the table that least SNR value is required to achieve the target outage value for our proposed method (SM-based DFTWR). For example, in case of 0.1 outage value, SM-based DFTWR requires 14 dB of SNR while PLNC requires 23 dB. As the outage value decreases, the gain in SNR for our proposed method is much more, which is beneficial. This is due to the fact that extra bits are used for activating the transmitting antenna thereby causing only one RF chain to be active at a time that reduces the interantenna interference. The SNR gain over PLNC is 8 dB while it is 3 dB over AFOWR for outage probability value of 0.03.

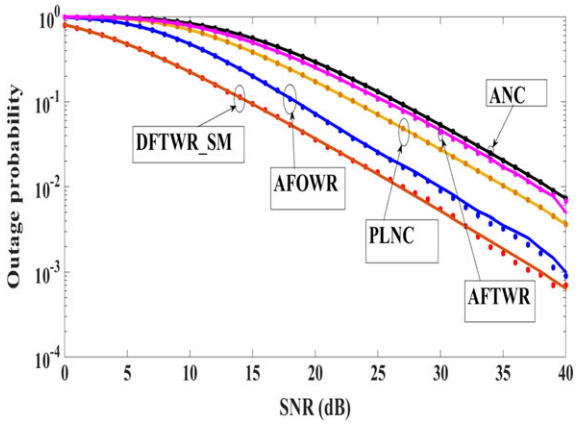

FIGURE 2 Outage probability analysis of the proposed and existing systems. (Solid line represents analytical results while ∗ sign indicates simulation results)

TABLE 3 Comparison of outage probability of different techniques

	SNR for Various Techniques, dB				
P_{out}	DFTWR_SM	AFOWR	PLNC	AFTWR	ANC
0.1	14	18	23	25	26
0.05	18	21	26	29	30
0.03	21	24	29	32	33

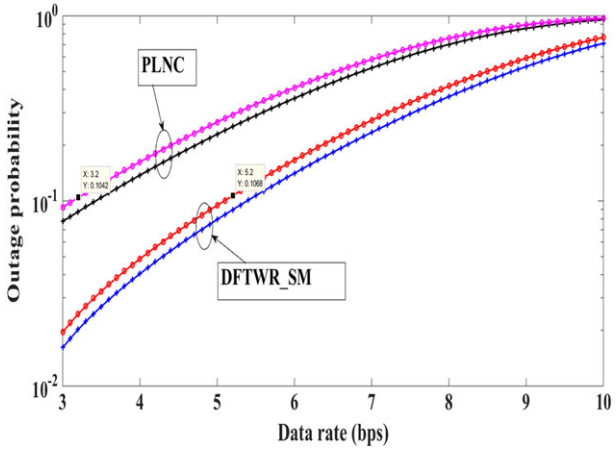

FIGURE 3 Upper bound on outage performance comparison between the proposed system and the existing PLNC system in terms of data rate. (+ sign indicates $\beta = 0$ while • sign indicates $\beta = 3$)

The upper bounds on outage performance of the new method and PLNC have been compared in Figure 3 analytically. The bounds show improvement in performance for SM-based DFTWR for both $\beta = 0$ and $\beta = 3$. $N = 2$ and $\eta_R = 40$ dB have been considered for this case. It can be seen that the proposed system has 2-bps data rate more than that of PLNC. This is due to the bits that are required for antenna selection, which in our case, is 1. Since the communication is full duplex, hence the increment factor will be 2. This can be explained with an example. For $\beta = 3$ and outage probability value of 0.1, PLNC has a data rate of 3.2 bps while SM-based DFTWR has a data rate of 5.2 bps.

For different SNR loss factors, $\beta = 0$ dB, $\beta = 3$ dB, and $\beta = 7$ dB, the lower bounds on outage probabilities have been shown in Figure 4. The target data rate is 3 bps, and the SNR at relay node is assumed to be equal to the SNR at source node. $N = 2$ has been considered for this case. It can be deduced from the graph that system performance is degraded by an increment in SNR loss factor because of the increase in interantenna interference. For example, for $\beta = 0$ dB and outage probability value of 0.01, SNR required is 26 dB, while, for $\beta = 3$ dB, SNR required is 27 dB and, for $\beta = 7$ dB, SNR required is 30 dB. We can observe that an increment in SNR loss factor also leads to a rise of the outage probability value.

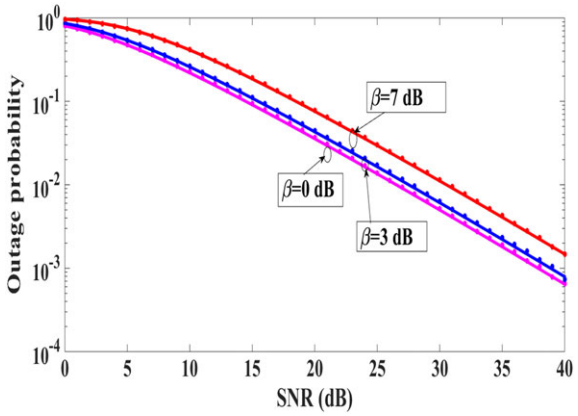

FIGURE 4 Lower bound of outage performance of the system with $\beta = 0$ dB, $\beta = 3$ dB, and $\beta = 7$ dB. (Solid line represents analytical results while + sign indicates simulation results)

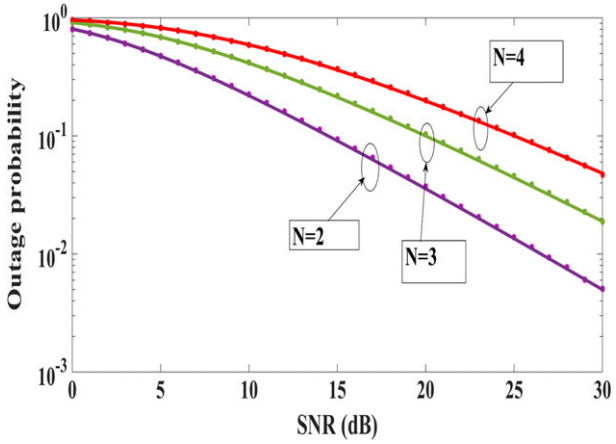

FIGURE 5 The impact of N on lower bound of outage performance. (Solid line represents analytical results while $*$ sign indicates simulation results)

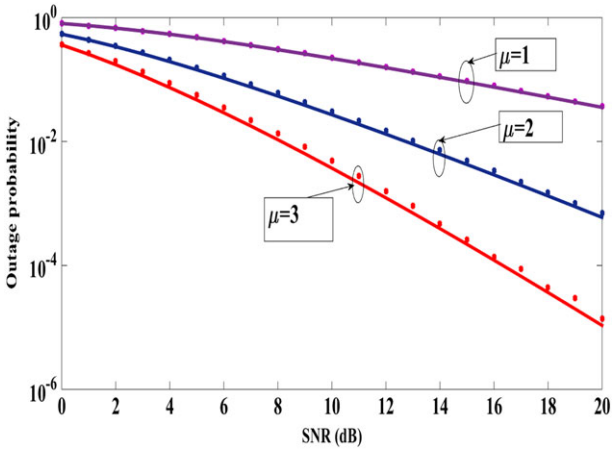

FIGURE 6 The impact of fading factor μ on lower bound of outage performance. (Solid line represents analytical results while $*$ sign indicates simulation results)

The lower bounds on outage probability have been plotted for various channel parameters like N, μ, κ, and α where the parameters have been defined earlier in Section 2. The impact on lower bounds of outage probability by varying N, μ, and α has been shown in Figures 5, 6, and 7, respectively. The impact of varying relative geometrical gain (κ) is depicted

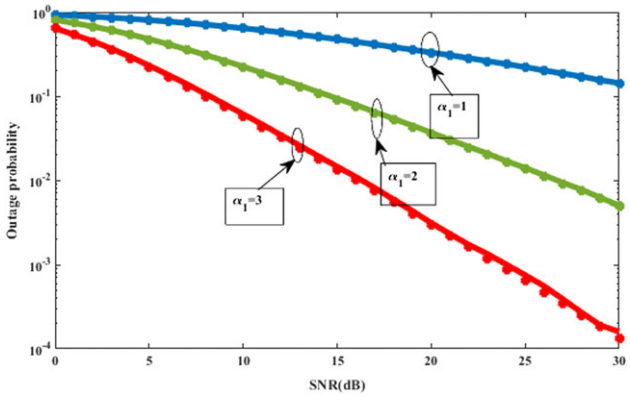

FIGURE 7 The effect of α_1 on lower bound of outage performance. (Solid line represents analytical results while $*$ sign indicates simulation results)

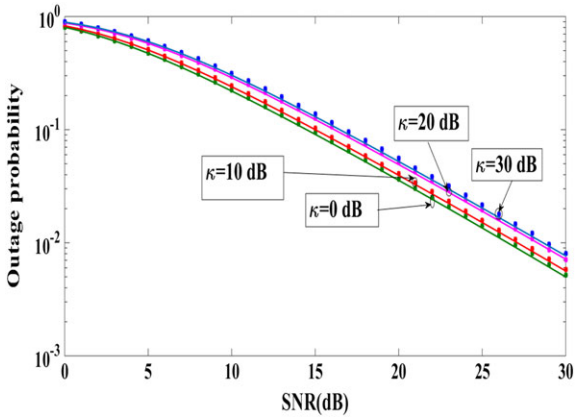

FIGURE 8 The impact of relative geometrical gain κ on lower bound of outage performance. (Solid line represents analytical results while $*$ sign indicates simulation results)

in Figure 8. SNR values at relay node, MR, and source nodes (MS1 and MS2) are considered to be equal, while $\beta = 0$ dB and $r = 1$ for all the cases. For Figure 5, the parameters are taken as data rate $(R) = 3$ bps, $\alpha_1 = 2$, $\mu = 1$, and $\kappa = 0$ dB for all links. For Figure 6, where variation of fading parameter (μ) is analyzed, the values are taken as $R = 3$ bps, $\alpha_1 = 2$, $N = 2$, and $\kappa = 0$ dB. For comparison of κ values, the remaining parameters are taken as $R = 3$ bps, $\mu = 1$, $N = 2$, and $\alpha_1 = 2$. In Figure 7, the parameters are $R = 3$ bps, $\mu = 1$, $\kappa = 0$ dB, and $N = 2$. It can be observed from Figure 5 that as the value of number of cascaded components (N) increases, the lower bound on outage probability increases resulting in degradation of system performance. This is due to the reason that fading increases with increment of N factor. A rise in μ value improves the system performance as displayed in Figure 6. Performance also improves with increase in value of α_1 as can be seen in Figure 7. The relay location is also varied, and its effects have been illustrated in Figure 8. From the graph, it is evident that $\kappa = 0$ dB provides the optimum performance. κ is varied between 0 to 30 dB with increments of 10 dB, ie, relay is brought much closer to MS1. Performance gradually worsens with increase in κ value.

The outage probability lower bound has been compared for different values of data rates in Figure 9. The values are taken as $\alpha_1 = 2$, $N = 2$, $\kappa = 0$ dB, $\eta_R = 40$ dB, $\beta = 0$ dB, and μ=1 for all links. As the target data rate value is increased, the outage probability increases resulting in inferior system performance. This is because achieving a higher data rate is difficult and may lead to more errors.

The average data rate of the proposed system has been compared with other algorithms, and the results have been plotted in Figure 10 after performing Monte Carlo simulations. The observation that can be drawn is that the proposed model outperforms PLNC. AFOWR performs the worst followed by ANC and PLNC. SM-based DFTWR has higher average data rate than AFTWR in case of lower SNR values where our proposed system is able to suppress the interantenna interference. However, as the SNR value crosses a certain threshold point, the interantenna interference dominates in case of SM-based DFTWR, and hence, AFTWR gives better average data rate than our proposed system.

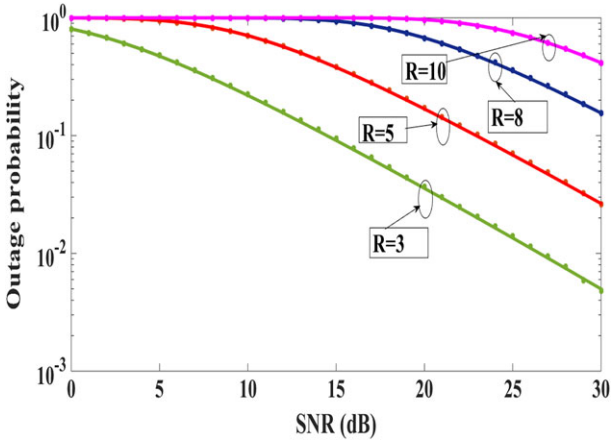

FIGURE 9 The impact of data rate R on outage performance. (Solid line represents analytical results while $*$ sign indicates simulation results)

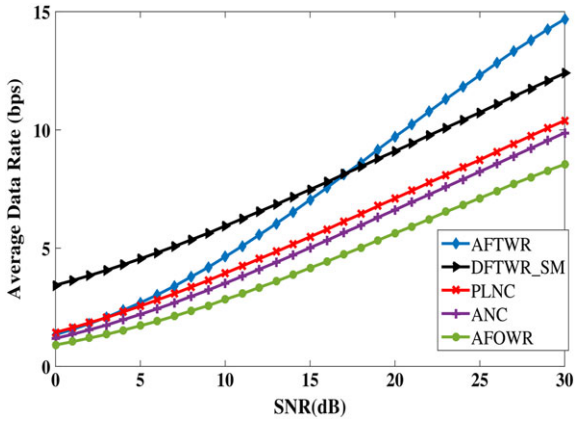

FIGURE 10 Simulation results for comparison of average data rate of various systems

6 | CONCLUSION

The analytical expressions for outage probability of SM-based DFTWR system has been derived and verified by implementing Monte Carlo simulations. The cascaded α-μ channel model has been utilized for this purpose. This system will be beneficial for D2D communication, where two devices located far away from each other can interact through a relay. The SM-based DFTWR system outperforms the systems available in literature. Also, it takes only two time slots to perform the SM-based DFTWR operation thereby doubling the efficiency of a conventional AF/DF system. The increase in system complexity for this method is compensated by the improvement in outage performance and data rate. The self-interference is mitigated because of the inherent network coding operation, thereby justifying the need for this method.

ORCID

Rakhesh Singh Kshetrimayum https://orcid.org/0000-0002-3383-2028

REFERENCES

1. Mumtaz S, Huq KMS, Rodriguez J. Direct mobile-to-mobile communication: paradigm for 5G. *IEEE Wirel Commun*. 2014;21(5):14-23.
2. Talha B, Patzold M. Channel models for mobile-to-mobile cooperative communication systems. *IEEE Veh Technol Mag*. 2011;6(2):33-43.
3. Paul BS, Hasan A, Madheshiya H, Bhattacharjee R. Time and angle of arrival statistics of mobile-to-mobile communication channel employing circular scattering model. *IETE J Res*. 2009;55(6):275-281.

4. Patzold M, Hogstad BO, Youssef N, Kim D. A MIMO mobile-to-mobile channel model: Part I—the reference model. In: IEEE 16th International Symposium on Personal, Indoor and Mobile Radio Communications; September 11; Berlin, Germany. 573-578. https://doi.org/10.1109/PIMRC.2005.1651501
5. Baltzis KB. A simplified geometric channel model for mobile-to-mobile communications. *Radio Eng*. 2011;20(4):961-967.
6. Samarasinghe PT, Lamahewa TA, Abhayapala TD, Kennedy RA. 3D mobile-to-mobile wireless channel model. In: Australian Communication Theory Workshop; February 2–5, 2010; Canberra, Australia. 30-34. https://doi.org/10.1109/AUSCTW.2010.5426757
7. Riaz M, Nawaz SJ, Khan NM. 3D ellipsoidal model for mobile-to-mobile radio propagation envrionments. *Wirel Pers Commun*. 2013;72(4):2465-2479.
8. Riaz M, Khan NM, Nawaz SJ. A generalized 3-D scattering channel model for spatiotemporal statistics in mobile-to-mobile communication environment. *IEEE Trans Veh Technol*. 2015;64(10):4399-4410.
9. Trigui I, Laourine A, Affes S, Stephenne A. On the performance of cascaded generalized K fading channels. In: Global Telecommunications Conference; December 1; Honolulu, HI, USA. 1-5. https://doi.org/10.1109/GLOCOM.2009.5426028
10. Salo J, Sallabi HR, Vainikainen P. The distribution of the product of independent Rayleigh random variables. *IEEE Trans Antennas Propag*. 2006;54(2):639-643.
11. Cheng X, Yang L, Shen X. D2D for intelligent transportation systems: a feasibility study. *IEEE Trans Intell Transp Syst*. 2015;16(4):1784-1793.
12. Leonardo EJ, Yacoub MD. Product of α-μ variates. *IEEE Wireless Commun Lett*. 2015;4(6):637-640.
13. Leonardo EJ, Yacoub MD. Statistics of the product of arbitary α-μ variates with applications. In: IEEE 25th International Symposium on Personal, Indoor and Mobile Radio Communications; September 2; Washington DC, USA. 73-76. https://doi.org/10.1109/PIMRC.2014.7136135
14. Gong FK, Ye P, Wang Y, Zhang N. Cooperative mobile-to-mobile communications over double Nakagami-m fading channels. *IET Commun*. 2012;6(18):3165-3175.
15. Xu LW, Zhang H, Lu TT, Gulliver TA. Performance analysis of the IAF relaying M2M cooperative networks over N-nakagami fading channels. *J Commun*. 2015;10(3):185-191.
16. Dias US, Yacoub MD. On the α-μ autocorrelation and power spectrum functions: field trials and validation. In: Proc. IEEE Global Telecommun. Conf.; December 1; Honolulu, HI, USA. 710-712. https://doi.org/10.1109/GLOCOM.2009.5425619
17. Wu Q, Matolak DW, Sen I. 5-GHz-band vehicle-to-vehicle channels: models for multiple values of channel bandwidth. *IEEE Trans Veh Technol*. 2010;59(5):2620-2625.
18. Karadimas P, Vagenas ED, Kotsopoulos SA. On the scatterers mobility and second order statistics of narrowband fixed outdoor wireless channels. *IEEE Trans Wireless Commun*. 2010;9(7):2119-2124.
19. Yilmaz F, Alouini MS. Product of the powers of generalized nakagami-m variates and performance of cascaded fading channels. In: IEEE Globecom; December 1; Honolulu, HI, USA. 1-8. https://doi.org/10.1109/GLOCOM.2009.5426254
20. Zhang S, Liew SC, Lam P. Hot topic: physical layer network coding. In: Annual International Conference on Information, Communications and Signal Processing; September 23; Los Angeles, CA, USA. 358-365. https://doi.org/10.1145/1161089.1161129
21. Liew SC, Zhang S. Physical-layer network coding: tutorial, survey and beyond. *Elsevier J Phys Commun*. 2013;6(3):4-42.
22. Chen P, Liew SC, Shi L. Bandwidth-efficient coded modulation schemes for physical-layer network coding with high-order modulations. *IEEE Trans Commun*. 2017;65(1):147-160. https://doi.org/10.1109/TCOMM.2016.2622693
23. Shi L, Yang T, Cai K, Chen P, Guo T. On MIMO linear physical-layer network coding: full-rate full-diversity design and optimization. *IEEE Trans Wirel Commun*. 2018;17(5):3498-3511. https://doi.org/10.1109/TWC.2018.2815621
24. Kong L, Chen P, Wang L. Outage probability analysis of a space-time block coding physical-layer network coding. In: 2012 International Conference on Wireless Communications and Signal Processing (WCSP); 2012:1-6. https://doi.org/10.1109/WCSP.2012.6542968
25. Yang K, Yang N, Xing C, Wu J. Relay antenna selection in MIMO two-way relay networks over Nakagami-m fading channels. *IEEE Trans Veh Technol*. 2014;63(5):2349-2362.
26. Nasab ES, Ardebilipour M. Multi-antenna AF-two way relaying over Nakagami-m fading channels. *Wirel Pers Commun*. 2013;73(3):717-729.
27. Amarasuriya G, Tellambura C, Ardakani M. Two-way amplify-and-forward multiple-input multiple-output relay networks with antenna selection. *IEEE J Sel Areas Commun*. 2012;30(8):1513-1529.
28. Zhang J, Li Q, Jin KK, Wang Y, Ge X. On the performance of full duplex two way relay channels with spatial modulation. *IEEE Trans Commun*. 2016;64(12).
29. Koc A, Altunbas I, Basar E. Two way full duplex spatial modulation systems with wireless powered AF relaying. *IEEE Wireless Commun Lett*; 7:444-447.
30. Gradshteyn IS, Ryzhik IM. *Table of Integrals, Series and Products*. New York, NY, USA: Academic Press; 1994.
31. Prudnikov AP, Brychkov YA, Marichev OI. *Integrals and Series: Special Functions, Additional Chapters*. Moscow, Russia: Fizmatlit Press; 2003.
32. Ilhan H, Uysal M, Altunbas I. Cooperative diversity of intervehicular communciation: performance analysis and optimization. *IEEE Trans Veh Technol*. 2009;58(7):3301-3310.
33. Ochiai H, Mitran P, Tarokh V. Variable-rate two-phase collaborative communication protocols for wireless networks. *IEEE Trans Veh Technol*. 2006;52(9):4299-4313.
34. Jiao B, Wen M, Ma M, Poor HV. Spatial modulated full duplex. *IEEE Wireless Commun Lett*. 2014;3(6):641-644. https://doi.org/10.1109/LWC.2014.2359218

35. Ju M, Kim M. Error performance analysis of BPSK modulation in physical-layer network-coded bidirectional relay networks. *IEEE Trans Commun*. 2010;58(10):2770-2775.
36. Shi Y, Ma M, Yang Y, Jiao B. Optimal power allocation in spatial modulation systems. *IEEE Trans Wirel Commun*. 2017;16(3):1646-1655. https://doi.org/10.1109/TWC.2017.2650905
37. Eslamifar M, Yuen C, Chin WH, Guan YL. Max-min antenna selection for bi-directional multi antenna relaying. In: IEEE Vehicular Technology Conference; May 16; Taipei, Taiwan. 1-5. https://doi.org/10.1109/VETECS.2010.5493619
38. Liu Y, Dharmawansa P, McKay MR. Max-flow min-cut characterization of dual-hop relay channels. In: Annual Allerton Conference on Communication, Control and Computing; October 1; Monticello, IL, USA. 1659-1665. https://doi.org/10.1109/Allerton.2012.6483421
39. Bhowal A, Kshetrimayum RS. End to end performance analysis of M2M cooperative communication over cascaded α-μ channels. In: IEEE COMSNETS; January 4; Bangalore, India. 211-224. https://doi.org/10.1109/COMSNETS.2017.7945366
40. Zhang Z, Ma Z, Ding Z, Xiao M, Karagiannidis GK. Full-duplex two way and one way relaying: average rate, outage probability and tradeoffs. *IEEE Trans Wirel Commun*. 2016;15(6):3920-3933.

How to cite this article: Bhowal A, Kshetrimayum RS. Outage probability bound of decode and forward two-way full-duplex relay employing spatial modulation over cascaded $\alpha - \mu$ channels. *Int J Commun Syst*. 2018;e3876. https://doi.org/10.1002/dac.3876